Journal of Power Sources 196 (2011) 7742–7746

Contents lists available at ScienceDirect

Journal of Power Sources

journal homepage: www.elsevier.com/locate/jpowsour

Short communication

$Ni_3(PO_4)_2$-coated $Li[Ni_{0.8}Co_{0.15}Al_{0.05}]O_2$ lithium battery electrode with improved cycling performance at 55 °C

Dong-Ju Lee[a,b], Bruno Scrosati[a,b,*], Yang-Kook Sun[a,c,**]

[a] Department of WCU Energy Engineering, Hanyang University, Seoul 133-791, South Korea
[b] Department of Chemistry, University of Rome Sapienza, 00185 Rome, Italy
[c] Department of Chemical Engineering, Hanyang University, Seoul 133-791, South Korea

ARTICLE INFO

Article history:
Received 26 January 2011
Received in revised form 3 April 2011
Accepted 4 April 2011
Available online 8 April 2011

Keywords:
Layered nickel-rich lithium cobalt oxide
Nickel phosphate coating: cathode material
Lithium cell
Lithium-ion battery

ABSTRACT

To improve the cycling performance of $LiNi_{0.8}Co_{0.15}Al_{0.05}O_2$ at 55 °C, a thin $Ni_3(PO_4)$ layer was homogeneously coated onto the cathode particle via simple ball milling. The morphology of the $Ni_3(PO_4)_2$-coated $LiNi_{0.8}Co_{0.15}Al_{0.05}O_2$ particle was characterized using SEM and TEM analysis, and the coating thickness was found to be approximately 10–20 nm. The $Ni_3(PO_4)_2$-coated $LiNi_{0.8}Co_{0.15}Al_{0.05}O_2$ cell showed improved lithium intercalation stability and rate capability especially at high C rates. This improved cycling performance was ascribed to the presence of $Ni_3(PO_4)_2$ on the $LiNi_{0.8}Co_{0.15}Al_{0.05}O_2$ particle, which protected the cathode from chemical attack by HF and thus suppressed an increase in charge transfer resistance. Transmission electron microscopy of extensively cycled particles confirmed that the particle surface of the $Ni_3(PO_4)_2$-coated $LiNi_{0.8}Co_{0.15}Al_{0.05}O_2$ remained almost undamaged, whereas pristine particles were severely serrated. The stabilization of the host structure by $Ni_3(PO_4)_2$ coating was also verified using X-ray diffraction.

1. Introduction

Layered composite Ni-rich $Li[Ni_{1-x}M_x]O_2$ (M = transition metal, $x \leq 0.2$) cathode materials are considered to be the most promising cathode materials for hybrid electric vehicles (HEVs), plug-in hybrid vehicles (PHEVs), and electric vehicles (EVs) due to their large capacity, excellent rate capability, and low cost [1–3]. Among the Ni-rich $Li[Ni_{1-x}M_x]O_2$ layered cathode materials, $LiNi_{0.8}Co_{0.15}Al_{0.05}O_2$ showed improved electrochemical and thermal stabilities by employing a stabilizing layered structure through the substitution of Co and Al for Ni sites, resulting in reduction of the *a*-axis. However, $LiNi_{0.8}Co_{0.15}Al_{0.05}O_2$ still showed capacity fading and resistance increase after storage and cycling tests at elevated temperatures above 55 °C due to the reactive and unstable Ni^{4+} ions in the delithiated $Li_{1-\delta}Ni_{0.8}Co_{0.15}Al_{0.05}O_2$ materials [4–6].

One way to enhance the electrochemical and thermal properties of Ni-rich $Li[Ni_{1-x}M_x]O_2$ cathode materials is to coat their surfaces with nanoscale layers of metal fluoride (AlF_3) and metal phosphate ($AlPO_4$) [6–9]. These nano-coating layers protect the highly delithiated cathode active materials from HF attack in the electrolyte, which greatly suppresses undesirable increases in interfacial resistance [6]. Recently, we reported that an AlF_3 coating on $LiNi_{0.8}Co_{0.15}Al_{0.05}O_2$ showed improved electrochemical and thermal properties. These improvements resulted in excellent storage performance at 60 °C, originating from the low and stable charge transfer resistance between the cathode and electrolyte and the suppression of surface degradation of the $LiNi_{0.8}Co_{0.15}Al_{0.05}O_2$ host structure by the AlF_3 coating [9].

Most coating work has been focused on wet processes that homogeneously coat the cathode particle surface, though at the expense of using a solvent and employing an additional heat-treatment step. Hence, the wet-coating process requires additional facilities and a solvent-treatment process, which lead to increased production cost for cathode active materials. Currently, dry-coating, direct coating of resistive materials (coating materials) onto the cathode particle surface, is the best method with regard to cost and process simplicity. However, the electrochemical performances of dry-coated cathode materials are generally inferior compared to those produced using wet-coating. Therefore, it is important to select good coating materials and an optimal coating process. Recently $(NH_4)_3AlF_6$-dry-coated $Li[Ni_{1/3}Co_{1/3}Mn_{1/3}]O_2$ and SiO_2-dry-coated $LiNi_{0.8}Co_{0.15}Al_{0.05}O_2$ showed remarkably enhanced cycling stabilities at an elevated temperature of 55 °C [10,11].

In the current study, $Ni_3(PO_4)_2$ is suggested and investigated as a coating material. A simple dry-coating of $Ni_3(PO_4)_2$ onto $LiNi_{0.8}Co_{0.15}Al_{0.05}O_2$ improved cycling stability at 55 °C com-

* Corresponding author at: Department of Chemistry, University of Rome Sapienza, 00185 Rome, Italy.
** Corresponding author at: Department of Chemical Engineering, Hanyang University, Seoul 133-791, South Korea.
E-mail address: bruno.scrosati@uniroma1.it (B. Scrosati).

0378-7753/$ – see front matter © 2011 Elsevier B.V. All rights reserved.
doi:10.1016/j.jpowsour.2011.04.007

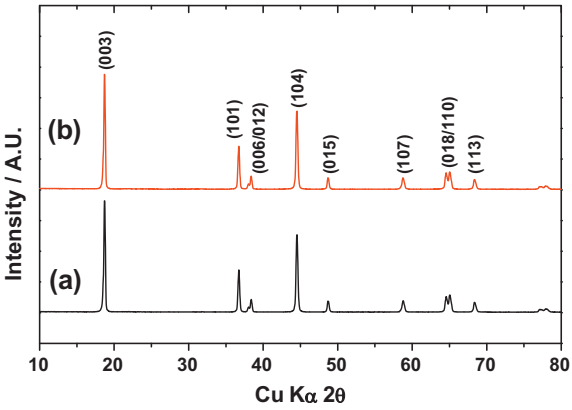

Fig. 1. XRD patterns of (a) pristine and (b) $Ni_3(PO_4)_2$-coated $LiNi_{0.8}Co_{0.15}Al_{0.05}O_2$ powders.

pared to that of the pristine material. We also elucidate the reason for the improvement in the electrochemical performance of the $Ni_3(PO_4)_2$-coated $LiNi_{0.8}Co_{0.15}Al_{0.05}O_2$ using electrochemical impedance spectroscopy (EIS) and transmission electron microscopy (TEM).

2. Experimental

Commercially available $LiNi_{0.8}Co_{0.15}Al_{0.05}O_2$ powder (Ecopro Co., Korea) was used as a pristine material. The $Ni_3(PO_4)_2$ powder was prepared through a co-precipitation reaction using aqueous solutions of $Ni(NO_3)_2{\cdot}6H_2O$, H_3PO_4 and NH_4OH at a molar ratio of 3:2:6 at a pH of 5.0. The three solutions were mixed thoroughly and aged for 12 h at 25 °C. The precipitate was filtered, washed, and dried at 100 °C for 12 h. To prepare $Ni_3(PO_4)_2$-coated $LiNi_{0.8}Co_{0.15}Al_{0.05}O_2$, 0.5 g of $Ni_3(PO_4)_2$ was mixed thoroughly with 100 g of $LiNi_{0.8}Co_{0.15}Al_{0.05}O_2$ powder via ball milling for 12 h at a speed of 100 rpm, and the obtained powder was heated at 500 °C for 5 h in air flow.

Powder X-ray diffraction (Rint-2000, Rigaku, Japan) measurements using Cu Kα radiation were employed to identify the crystalline phases of the synthesized powders. The surface of the $Ni_3(PO_4)_2$-coated powder was also observed using a scanning electron microscope (SEM, S-4800, HITACHI) and transmission electron microscopy (TEM, JEOL 2010). AC impedance measurements were performed using a Zahner Elektrik IM6 impedance analyzer over the frequency range of 1 MHz to 1 mHz with an amplitude of 10 mV rms.

Electrochemical testing was performed in 2032 coin-type cells. The positive electrodes were fabricated by blending the prepared powders, Super P carbon black, and polyvinylidene fluoride (85:7.5:7.5) in N-methyl-2-pyrrolidone. The slurry was then cast onto aluminum foil and dried at 110 °C for 10 h in a vacuum oven, at which time disks were punched out of the foil. The negative electrode was lithium foil, and the electrolyte was a 1 M $LiPF_6$ solution in an ethylene carbonate (EC)–diethyl carbonate (DEC) mixture (1:1 ratio by volume, PANAX ETEC Co., Korea). The positive and negative electrodes were separated by a porous polypropylene film. All cells were prepared in an Ar-filled dry box and were charged and discharged within a voltage range of 2.7–4.3 V at a constant current density of 0.5 C (100 mA g^{-1}) and elevated temperature (55 °C).

3. Results and discussion

Fig. 1 shows the XRD patterns of the pristine and $Ni_3(PO_4)_2$-coated $LiNi_{0.8}Co_{0.15}Al_{0.05}O_2$ powders, exhibiting a typical layered hexagonal structure without any impurity phases. The lattice constants of the $Ni_3(PO_4)_2$-coated $LiNi_{0.8}Co_{0.15}Al_{0.05}O_2$ powder were $a = 2.864(2)$ and $c = 14.194(5)$ Å, as calculated by a least squares method. These values are close to those of the pristine material, $a = 2.863(8)$ and $c = 14.191(4)$ Å, implying that the $Ni_3(PO_4)_2$ was not incorporated into the $LiNi_{0.8}Co_{0.15}Al_{0.05}O_2$ host structure, as no changes were seen in the lattice constants.

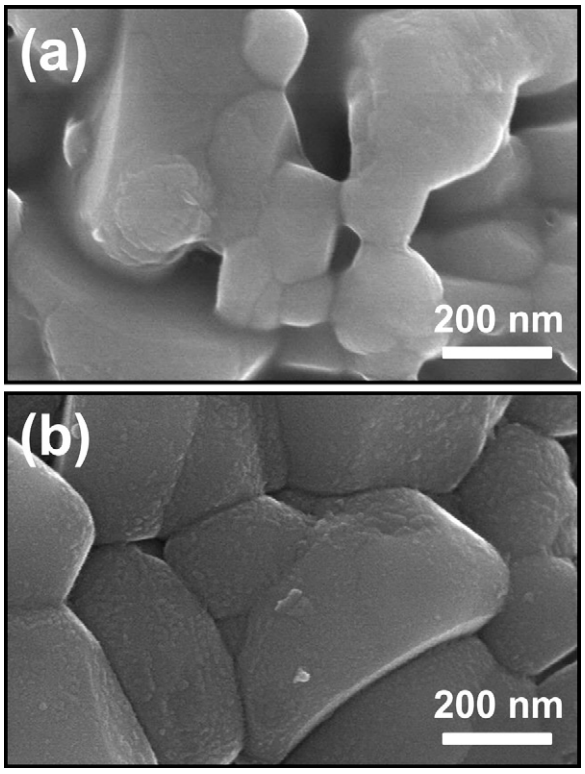

Fig. 2. SEM images of (a) pristine and (b) $Ni_3(PO_4)_2$-coated $LiNi_{0.8}Co_{0.15}Al_{0.05}O_2$ powders.

Fig. 2 shows SEM images of pristine and $Ni_3(PO_4)_2$-coated $LiNi_{0.8}Co_{0.15}Al_{0.05}O_2$ powders. The surfaces of the pristine $LiNi_{0.8}Co_{0.15}Al_{0.05}O_2$ particles are clean and smooth. After $Ni_3(PO_4)_2$ coating, as seen in Fig. 2(b), 10–20-nm-sized $Ni_3(PO_4)_2$ particles were homogeneously coated onto the surfaces of $LiNi_{0.8}Co_{0.15}Al_{0.05}O_2$ particles. This uniform $Ni_3(PO_4)_2$ coating was expected to improve cycling performance by protecting the $LiNi_{0.8}Co_{0.15}Al_{0.05}O_2$ particle surfaces.

To estimate the thickness of the $Ni_3(PO_4)_2$ coating layer, pristine and coated particles were examined using TEM. As shown in Fig. 3b, a nanoscale $Ni_3(PO_4)_2$ layer with a thickness of 20 nm was coated homogeneously onto the surface of the $LiNi_{0.8}Co_{0.15}Al_{0.05}O_2$ particles. As expected, the bright field TEM of a pristine $LiNi_{0.8}Co_{0.15}Al_{0.05}O_2$ particle shown in Fig. 3a did not have an extra film on the particle surface.

Fig. 4a shows the initial charge/discharge curves of Li/pristine and $Ni_3(PO_4)_2$-coated $LiNi_{0.8}Co_{0.15}Al_{0.05}O_2$ cells after application of a constant current density of 40 mA g^{-1} (0.2 C) between 2.7 and 4.3 V at 55 °C. Both cells showed very smooth charge/discharge curves, and the curves for both cells were nearly identical even up to the cut-off voltage of 4.3 V. The $Ni_3(PO_4)_2$-coated $LiNi_{0.8}Co_{0.15}Al_{0.05}O_2$ delivered a discharge capacity of 205 mAh g^{-1}, while the pristine electrode showed a slightly lower capacity of 203 mAh g^{-1}. This result implies that the coating medium of $Ni_3(PO_4)_2$ does not act as a barrier for Li^+ transportation.

To investigate the effectiveness of the surface modification, the two materials were cycled at a current rate of 100 mA g^{-1} (0.5 C) and at 55 °C. Fig. 4b exhibits discharge capacity versus cycle num-

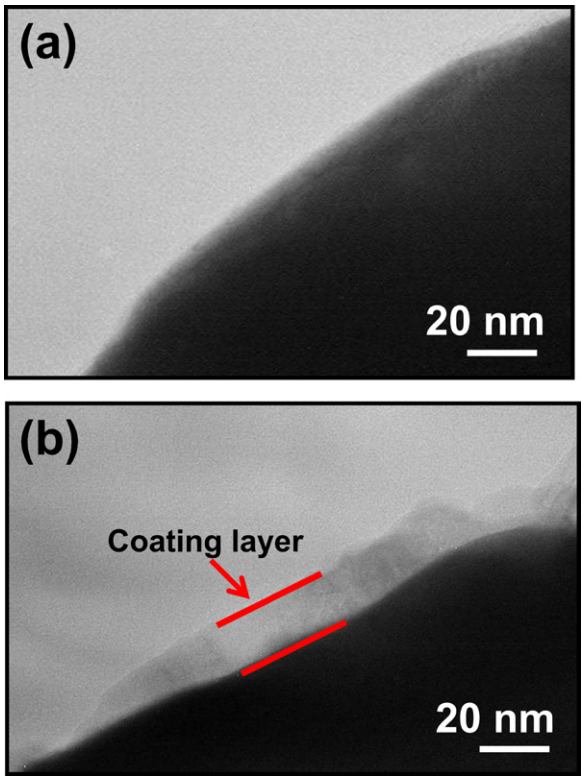

Fig. 3. TEM bright-field images of (a) pristine and (b) $Ni_3(PO_4)_2$-coated $LiNi_{0.8}Co_{0.15}Al_{0.05}O_2$ particles.

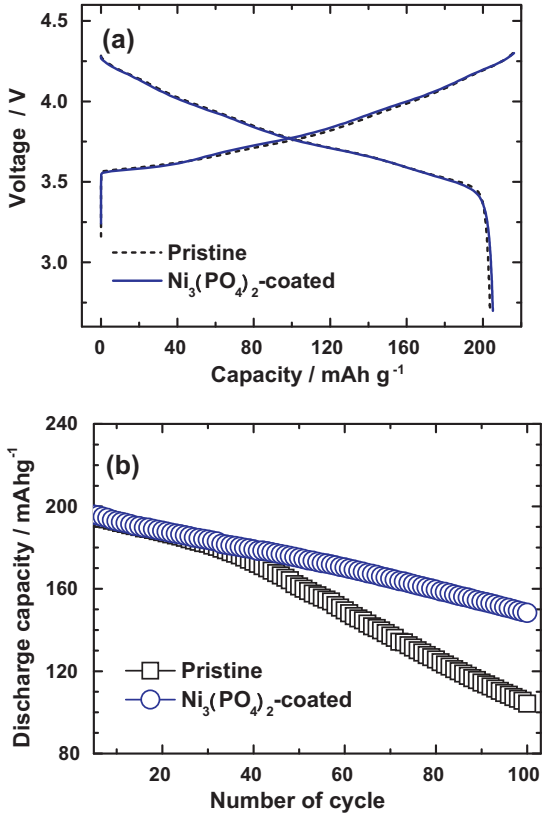

Fig. 4. (a) Initial charge–discharge curves of Li/pristine and Li/$Ni_3(PO_4)_2$-coated $LiNi_{0.8}Co_{0.15}Al_{0.05}O_2$ cells at a current density of 40 mA g^{-1} (0.2 C) between 3.0 V and 4.3 V. (b) Variations in discharge capacity of Li/pristine and Li/$Ni_3(PO_4)_2$-coated $LiNi_{0.8}Co_{0.15}Al_{0.05}O_2$ cells at a current density of 100 mA g^{-1} (0.5 C).

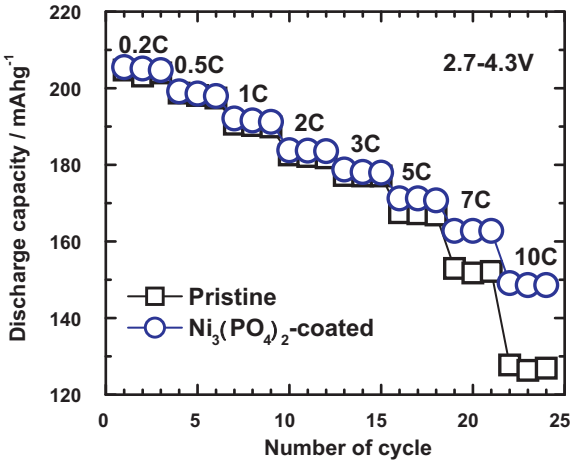

Fig. 5. Rate capability test of pristine and $Ni_3(PO_4)_2$-coated $LiNi_{0.8}Co_{0.15}Al_{0.05}O_2$ cells as a function of C rate.

ber for the Li/pristine and $Ni_3(PO_4)_2$-coated $LiNi_{0.8}Co_{0.15}Al_{0.05}O_2$ cells between 2.7 and 4.3 V. The initial discharge capacity of the $Ni_3(PO_4)_2$-coated $LiNi_{0.8}Co_{0.15}Al_{0.05}O_2$ was 198 mAh g^{-1}, while that of the pristine sample was 197 mAh g^{-1}. However, the cycling behavior of the $Ni_3(PO_4)_2$-coated $LiNi_{0.8}Co_{0.15}Al_{0.05}O_2$ greatly improved, showing a capacity retention of 75% after 100 cycles, while the pristine electrode showed a gradual decrease in capacity, leading to a capacity retention of only 53% during the same cycling period.

Fig. 5 shows the discharge capacities of Li/pristine and $Ni_3(PO_4)_2$-coated $LiNi_{0.8}Co_{0.15}Al_{0.05}O_2$ cells as a function of C rate (1 C corresponds to 200 mA g^{-1}) between 2.7 and 4.3 V. The cells were charged galvanostatically with a current density of 0.2 C (40 mA g^{-1}) before each discharge and were then discharged at a C rate from 0.2 C to 10 C (2000 mA g^{-1}). As observed in Fig. 5, the two materials showed similar electrochemical performances at low C rate. However, with increasing C rate, $Ni_3(PO_4)_2$-coated $LiNi_{0.8}Co_{0.15}Al_{0.05}O_2$ delivered a higher discharge capacity than did the pristine material. For instance, the discharge capacity of $Ni_3(PO_4)_2$-coated $LiNi_{0.8}Co_{0.15}Al_{0.05}O_2$ at a 10 C rate was 149 mAh g^{-1}, while the pristine $LiNi_{0.8}Co_{0.15}Al_{0.05}O_2$ delivered only 127 mAh g^{-1}. This result encourages us to believe that the $Ni_3(PO_4)_2$ coating layer on $LiNi_{0.8}Co_{0.15}Al_{0.05}O_2$ does not block a Li^+ intercalation but rather functions as an expediter for Li^+ transport to the host structure as a result of the reduced interfacial resistance between the cathode and the electrolyte [6].

Electrochemical impedance spectroscopy (EIS) was performed to investigate the improved electrochemical performance of the $Ni_3(PO_4)_2$-coated $LiNi_{0.8}Co_{0.15}Al_{0.05}O_2$ in a charged state of 4.3 V as a function of cycle number at 55 °C. Fig. 6 shows Nyquist plots of the pristine and $Ni_3(PO_4)_2$-coated $LiNi_{0.8}Co_{0.15}Al_{0.05}O_2$ after 1, 25, 50, and 100 cycles. Expanded views in the inset depict the high-to-medium frequency region. The equivalent circuit used in this study was reported in our previous study [10]. The high-to-medium frequency semicircle was attributed to the resistance of the surface film (R_{sf})-covered electrode particles, and the low-frequency was attributed to the charge transfer resistance (R_{ct}) at the interface between the electrode and electrolyte. The R_{sf} for both the electrodes was relatively small compared to R_{ct} and remained stable at 35–45 Ω during cycling, implying that the $Ni_3(PO_4)_2$ coating layer had no effect on the surface film resistance, as discussed above. Notice that R_{ct} for both electrodes rapidly increased with cycling; the R_{ct} value of the pristine $LiNi_{0.8}Co_{0.15}Al_{0.05}O_2$ after 1 cycle was 258.8 Ω, increasing to 1039.7 Ω after 100 cycles. On the contrary, the R_{ct} of the $Ni_3(PO_4)_2$-coated $LiNi_{0.8}Co_{0.15}Al_{0.05}O_2$

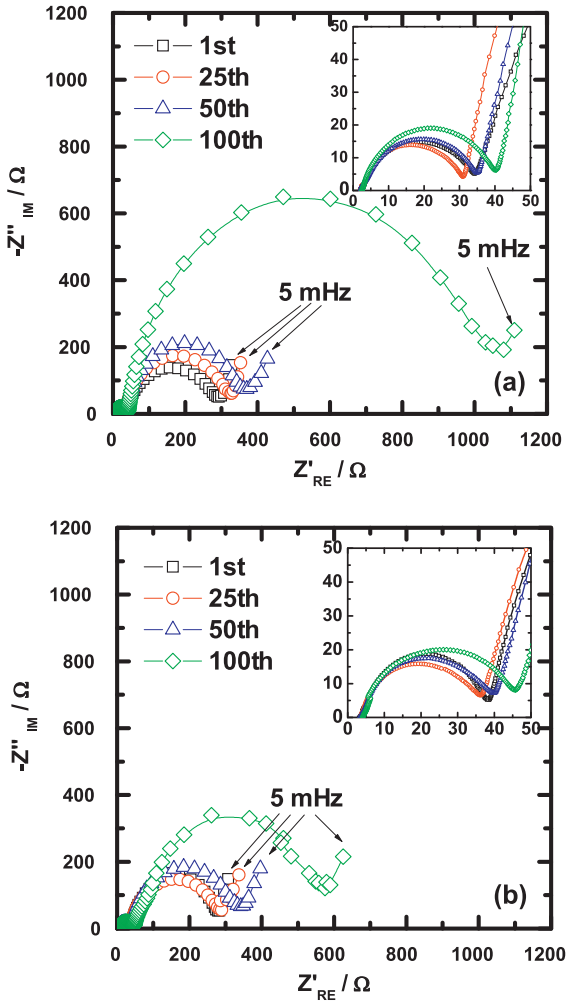

Fig. 6. Nyquist plots of (a) pristine and (b) $Ni_3(PO_4)_2$-coated $LiNi_{0.8}Co_{0.15}Al_{0.05}O_2$ cells at the 1st, 25th, 50th, and 100th cycles.

electrode was initially somewhat lower, 240.6 Ω after 1 cycle, and only increased to 529.2 Ω after 100 cycles. Similar phenomena were previously reported for AlF_3-coated $LiNi_{0.8}Co_{0.15}Al_{0.05}O_2$ and $Li[Ni_{0.8}Co_{0.1}Mn_{0.1}]O_2$ [6,10] due to suppression of the surface degradation of the host structure using an AlF_3 coating. Increased R_{ct} during cycling indicates the formation of surface films such as LiF and Li_xPF_y- and $Li_xPF_yO_z$-type compounds which are highly resistive to Li^+ migration [12]. Based on these results, we believe that $Ni_3(PO_4)_2$ coating layers are helpful for inhibiting the chemical reaction between the highly delithiated $Li_{1-\delta}Ni_{0.8}Co_{0.15}Al_{0.05}O_2$ and the electrolyte.

Fig. 7 shows the XRD patterns of extensively cycled pristine and $Ni_3(PO_4)_2$–$LiNi_{0.8}Co_{0.15}Al_{0.05}O_2$ electrodes after 100 cycles at 55 °C. An Al current collector and graphite were used as the inner standard to calibrate the diffraction patterns. Both the pristine and $Ni_3(PO_4)_2$-coated $LiNi_{0.8}Co_{0.15}Al_{0.05}O_2$ maintained the original hexagonal layer α-$NaFeO_2$ structure. The intensity ratio of I_{003}/I_{104} is reported to be closely related to the undesirable cation mixing between Li^+ and Ni^{2+}, which is reduced as the ratio is increased [13]. The intensity of I_{003}/I_{104} decreased from 1.22 for the $Ni_3(PO_4)_2$-coated $LiNi_{0.8}Co_{0.15}Al_{0.05}O_2$ to 1.15 for the pristine electrode, compared to 1.44 for the fresh $LiNi_{0.8}Co_{0.15}Al_{0.05}O_2$ powder, indicating that the $Ni_3(PO_4)_2$ coating maintains the structural stability of $LiNi_{0.8}Co_{0.15}Al_{0.05}O_2$ host structure.

Fig. 8 shows SEM images of the pristine and the $Ni_3(PO_4)_2$-coated $LiNi_{0.8}Co_{0.15}Al_{0.05}O_2$ particle surfaces after 100 cycles at

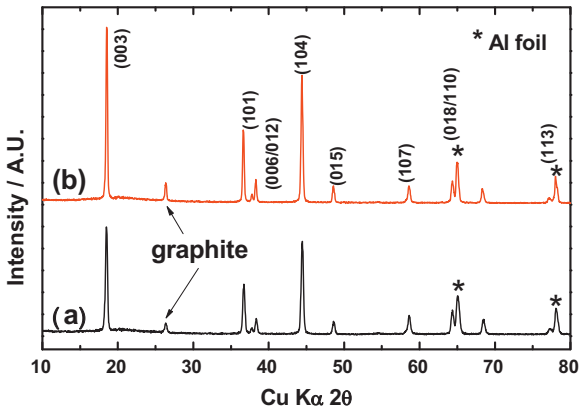

Fig. 7. XRD spectra of (a) pristine and (b) $Ni_3(PO_4)_2$-coated $LiNi_{0.8}Co_{0.15}Al_{0.05}O_2$ electrodes after 100 cycles at 55 °C.

55 °C. Though the surfaces of both samples were covered with an SEI layer during prolonged cycling [14], the morphologies of the two samples were quite different from one another. The surfaces of the pristine $LiNi_{0.8}Co_{0.15}Al_{0.05}O_2$ particles were severely damaged, and the exteriors of primary particles was serrated compared to those of $Ni_3(PO_4)_2$-coated $LiNi_{0.8}Co_{0.15}Al_{0.05}O_2$.

To observe the surface morphological changes of $LiNi_{0.8}Co_{0.15}Al_{0.05}O_2$ particles in detail, both the cycled electrodes after 100 cycles at 55 °C were characterized using high resolution TEM. Fig. 9a shows a TEM image of a cycled pristine $LiNi_{0.8}Co_{0.15}Al_{0.05}O_2$ particle. The particle was severely damaged, and the edge of the primary particle was serrated, whereas the fresh materials exhibited a smooth particle surface (Fig. 3a). We believed that the metal (Ni and Co) dissolution from the highly delithiated $Li_{1-\delta}Ni_{0.8}Co_{0.15}Al_{0.05}O_2$ particles gave rise to the serrated particles

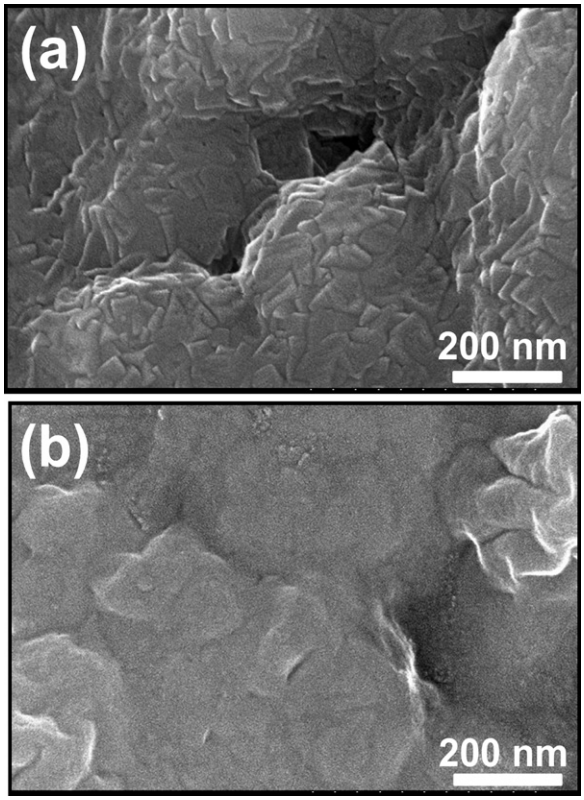

Fig. 8. SEM images of (a) pristine and (b) $Ni_3(PO_4)_2$-coated $LiNi_{0.8}Co_{0.15}Al_{0.05}O_2$ powders after 100 cycles at 55 °C.

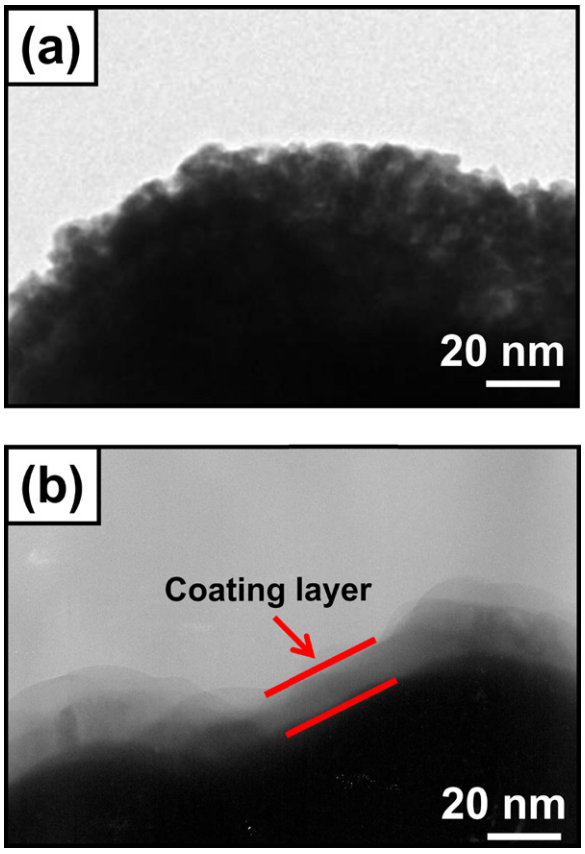

Fig. 9. Bright field TEM images of cycled (a) pristine and (b) $Ni_3(PO_4)_2$-coated $LiNi_{0.8}Co_{0.15}Al_{0.05}O_2$ electrodes after 100 cycles at 55 °C.

[10], which contributed significantly to the high charge-transfer resistance observed for the pristine $LiNi_{0.8}Co_{0.15}Al_{0.05}O_2$ electrode, as shown in Fig. 6a. On the contrary, the $Ni_3(PO_4)_2$-coated $LiNi_{0.8}Co_{0.15}Al_{0.05}O_2$ particles still show smooth $Ni_3(PO_4)_2$ coating layers, and thus the coated particle has a distinct, smooth edge, see Fig. 9b

4. Conclusions

$LiNi_{0.8}Co_{0.15}Al_{0.05}O_2$ particles were coated with a uniform and thin $Ni_3(PO_4)_2$ layer with a thickness of 10–20 nm using a simple dry ball-milling method. The $Ni_3(PO_4)_2$-coated $LiNi_{0.8}Co_{0.15}Al_{0.05}O_2$ exhibited greatly improved lithium intercalation stability, having a capacity retention of 73% after 100 cycles at 55 °C, while that of pristine material was only 53%. This improvement originated from the stable charge transfer resistance between cathode and electrolyte and suppression of surface degradation and bulk structure formation due to protection of the $LiNi_{0.8}Co_{0.15}Al_{0.05}O_2$ by the $Ni_3(PO_4)_2$ coating.

Although here we do not report specific tests, e.g., metal solubility, comparison of the electrochemical response of our coated electrode with that of a pristine one, ICP and/or XPS for metal deposition on the electrode surface due to HF attack and dissolution, some previous results obtained in our laboratory, supported by pertinent literature works, make us confident in affirming the stability of our coated material. In a recent paper we tested the Ni, Co, and Mn solubility from a $Li[Ni_{0.55}Co_{0.15}Mn_{0.30}]O_2$ electrode material [15] and showed that, despite the fact that a large amount of Ni dissolution was observed, the $Li[Ni_{0.55}Co_{0.15}Mn_{0.30}]O_2$ electrode still exhibited a high capacity of 196 mAh g^{-1} with good cycle life keeping 93% of initial capacity after 50 cycles. As it is well known, quite different is the behavior of the spinel $LiMn_2O_4$ electrode, either in the pristine state or stabilized by aluminum, i.e., $Li_{1.1}Al_{0.05}Mn_{1.85}O_4$: the cells formed by combining this cathode with a graphite anode show a very poor cycle and calendar life, especially at elevated temperatures, due to the breakdown of the solid electrolyte interface (SEI) caused by Mn dissolution [16]. On the contrary, the capacity fade of NCA/C cells is mainly due to phase transition of the NCA layered structure [17]. We believe that this applies also to our layered material and accordingly, that its stability will not be jeopardized, even if Ni and Co dissolution may eventually occur.

It is also important to point out that this work reports a study specifically addressed to the characterization of the single electrode. We plan to investigate the behavior of a full cell by combining the coated $LiCoNiAlO_2$ cathode with a graphite anode. The evaluation of the cell response at 55 °C and of the nature of the SEI layer forming on the surface of the cathode will be part of this future study.

Acknowledgements

This work was supported by the Human Resources Development of the Korea Institute of Energy Technology Evaluation and Planning (KETEP) grant funded by the Korea government Ministry of Knowledge Economy (No. 20104010100560), and by the WCU (World Class University) program through the Korea Science and Engineering Foundation by Education, Science, and Technology (R31-2008-000-10092).

References

[1] J. Shim, R. Kostecki, T. Richardson, X. Song, K.A. Striebel, J. Power Sources 112 (2002) 222.
[2] R. Kostecki, F. McLarnon, Electrochem. Solid State Lett. 7 (2004) A380.
[3] M.-H. Kim, H.-S. Shin, D. Shin, Y.-K. Sun, J. Power Sources 159 (2006) 1328.
[4] H. Kondo, Y. Takeuchi, T. Sasaki, S. Kawauchi, Y. Itou, O. Hiruta, C. Okuda, M. Yonemura, T. Kamiyama, Y. Ukyo, J. Power Sources 174 (2007) 1131.
[5] D.P Abraham, R.D. Twesten, M. Balasubramanian, I. Petrov, J. McBreen, K. Amine, Electrochem. Commun. 4 (2002) 620.
[6] S.-U. Woo, C.S. Yoon, K. Amine, I. Belharouak, Y.-K. Sun, J. Electrochem. Soc. 154 (2007) A1005.
[7] J. Cho, T.-J. Kim, J. Kim, M. Noh, B. Park, J. Electrochem. Soc. 151 (2004) A1899.
[8] H.-B. Kim, B.-C. Park, S.-T. Myung, K. Amine, J. Prakash, Y.-K. Sun, J. Power Sources 179 (2008) 347.
[9] B.-C Park, H.-B. Kim, H.J. Bang, J. Prakash, Y.-K. Sun, Ind. Eng. Chem. Res. 47 (2008) 3876.
[10] Y.-K. Sun, S.-T. Myung, C.S. Yoon, D.-W. Kim, Electrochem. Solid-State Lett. 12 (2009) A163.
[11] Y. Cho, J. Cho, J. Electrochem. Soc. 157 (2010) A625.
[12] D. Aurbach, B. Markovsky, K. Gamolsky, E. Levi, Y. Ein-Eli, Electrochim. Acta 45 (1999) 67.
[13] T. Ohzuku, A. Ueda, M. Nagayama, Y. Iwakoshi, H. Komori, Electrochim. Acta 38 (1993) 1159.
[14] K. Edstrom, T. Gustafsson, J.O. Thomas, Electrochim. Acta 50 (2004) 397.
[15] B.R. Lee, et al., J. Electrochem. Soc. 158. (2011) A180.
[16] K. Amine, et al., J. Power Sources 129 (2004) 14.
[17] H. Kondo, et al., J. Power Sources 174 (2007) 1131.